Science & Technology Development Journal, 25(1):2342-2353

Open Access Full Text Article

Research Article

On the amplitude dynamics of solitons in waveguide systems with the generic Kerr nonlinearity coefficient and nonlinear gain-loss

Toan T. Huynh[1,2,*]

Use your smartphone to scan this QR code and download this article

ABSTRACT

We study the transmission of optical solitons in a nonlinear waveguide with the generic Kerr nonlinearity coefficient, the frequency dependent linear gain-loss, and the Ginzburg-Landau (GL) gain-loss profile. We first derive the expression for the collision-induced amplitude dynamics of two fast single solitons in the presence of weak cubic loss and weak quintic loss. This expression is then used to study the amplitude dynamics of solitons in multichannel optical waveguide systems. We show that the dynamics of soliton amplitudes in two-sequence transmission with the GL gain-loss profile are described by a Lotka-Volterra (LV) model. The stability analysis for the LV model is used to obtain the simple conditions on the physical parameters and to calculate the linear amplifier gain-loss for the transmission stabilization of the soliton sequences. The theoretical calculations are then confirmed by numerical simulations with the corresponding nonlinear Schrödinger (NLS) models. Furthermore, the optimal value of the Kerr nonlinearity coefficient for the robust transmission stabilization of the soliton sequences with the GL gain-loss profile is also proposed.

Key words: Soliton, Nonlinear Schrödinger equation, Kerr nonlinearity, Amplitude dynamics, Transmission stabilization, Multichannel optical waveguide transmission

[1]*Department of Mathematics, University of Medicine and Pharmacy at Ho Chi Minh City, Ho Chi Minh City, Vietnam*

[2]*Faculty of Mathematics and Computer Science, University of Science, Vietnam National University-HCMC, Ho Chi Minh City, Vietnam*

Correspondence

Toan T. Huynh, Department of Mathematics, University of Medicine and Pharmacy at Ho Chi Minh City, Ho Chi Minh City, Vietnam

Faculty of Mathematics and Computer Science, University of Science, Vietnam National University-HCMC, Ho Chi Minh City, Vietnam

Email: huynhthanhtoan@ump.edu.vn

History

- Received: 2021-09-03
- Accepted: 2021-12-12
- Published: 2021-3-31

DOI : 10.32508/stdj.v25i1.3808

INTRODUCTION

Solitons are the stable shape preserving traveling-wave solutions of nonlinear wave models such as the NLS model, the GL model, or the Korteweg-de Vries (KdV) model[1–7]. Recently, solitons have attracted much attention in a variety of fields, including hydrodynamics, condensed matter physics, and optics[4–7]. In nonlinear optical media, solitons, which can be described by the NLS equations, are formed thanks to the perfect balance between nonlinearity and dispersion[4–6]. One of the most fundamental properties of solitons is elastic collision, *i.e.*, the fact that solitons do not change their shape in collisions[4–6]. Due to the stability of solitons of NLS equations, they can be used as bits of information and can be extensively used in the information transmission and processing in broadband waveguide systems[4,5]. Through broadband optical waveguide links, the information transmission rate can be significantly increased based on the wavelength-division-multiplexing (WDM) method, where many pulse sequences propagate through the same waveguide[4,5,8]. In these systems, each pulse sequence is characterized by the central frequency of its pulses and is called a frequency channel. WDM or multichannel systems have been the subject of intensive research in recent decades due to their important applications in fiber optics transmission lines[5,8], data transfer between computer processors[9,10], and multiwavelength lasers[11,12].

In this paper, we consider the transmission of two soliton sequences in a broadband optical waveguide system with a large frequency difference between two sequences. We take into account the effects of the second-order dispersion, the linear gain-loss, the GL gain-loss profile, and Kerr nonlinearity with the generic Kerr nonlinearity coefficient γ. The propagation is described by the following system of coupled perturbed NLS equations[13–16]:

$$\begin{aligned} &i\partial_z\psi_i+\partial_t^2\psi_i+\gamma\left|\psi_j\right|^2\psi_j+2\gamma\left|\psi_k\right|^2\psi_j= \\ &iF^{-1}\left[\widehat{g}_j(\omega)\,\widehat{\psi}_j\right]/2+i\varepsilon_3\left|\psi_j\right|^2\psi_j+2i\varepsilon_3\left|\psi_k\right|^2\psi_j \\ &-i\varepsilon_5\left|\psi_j\right|^4\psi_j-3i\varepsilon_5\left|\psi_k\right|^4\psi_j \\ &-6i\varepsilon_5\left|\psi_k\right|^2\left|\psi_j\right|^2\psi_j, \end{aligned} \quad (1)$$

where $1\le j,\ k\le 2$ with $j\ne k$ and ψ_j is proportional to the envelope of the soliton sequence j. In Eq. (1), z is the propagation distance, t is the time, ε_3 and ε_5 are the cubic gain and quintic loss coefficients, respectively, with $0<\varepsilon_3,\ \varepsilon_5\square\ 1$, F^{-1} is the inverse Fourier transform, $\widehat{\psi}_j$ is the Fourier transform of ψ_j with respect to t, and $\widehat{g}_j(\omega)$ corresponds to the linear gain-loss[4,16,17]. On the left-hand side of Eq. (1), the second term corresponds to the second-order dispersion, while the third and last terms describe the

Cite this article : Huynh T T. **On the amplitude dynamics of solitons in waveguide systems with the generic Kerr nonlinearity coefficient and nonlinear gain-loss**. *Sci. Tech. Dev. J.;* 25(1):2342-2353.

intrasequence and intersequence interaction due to Kerr nonlinearity. On the right-hand side of Eq. (1), the first term is due to the linear gain-loss, the second and third terms describe the effects of intrasequence and intersequence interaction due to cubic gain, while the fourth, fifth, and last terms describe the effects of intrasequence and intersequence interaction due to quintic loss.

It is well known that the propagation of solitons in silicon waveguides can be affected by nonlinear loss, which arises due to gain or loss saturation or multi-photon absorption (MPA) [13,18–20]. This can lead to a downshift of the soliton amplitude and frequency in a two-soliton collision. The expressions for the collision-induced amplitude shift in fast collisions of two solitons with Kerr nonlinearity coefficient γ = 2 were derived in Refs. [16,18,21] for cubic loss and in Ref. [13] for quintic loss. The LV models were also established to study the amplitude dynamics of soliton sequences with cubic loss in Ref. [13] and with the GL gain-loss profile in Refs. [13,14,16,22] for γ = 2. However, the expression for the collision-induced amplitude shift of two solitons with nonlinear loss and a reduced model for deterministic amplitude dynamics due to the GL gain-loss profile have not been uncovered for the generic Kerr nonlinearity coefficient. Furthermore, the use of the frequency dependent linear gain-loss $\widehat{g}_j(\omega)$ for investigating the propagation stabilization of solitons has been studied in several earlier works, such as in Ref. [23] with delayed Raman response for γ = 2 and in Ref. [15] for the generic coefficient γ. In these papers, it has been shown that the use of the frequency dependent linear gain-loss $\widehat{g}_j(\omega)$ can suppress radiative effects via the decay of the radiative sidebands and lead to the enhancement of the propagation stabilization of solitons at long distances compared to the use of the constant gain-loss coefficients. However, the robustness of the use of the frequency-dependent linear gain-loss for stabilizing the propagation of soliton sequences in the presence of the GL gain-loss profile with the generic coefficient γ has not been studied. In particular, the investigations for the optimal value γ in the transmission stability of soliton sequences with the GL gain-loss profile have not been explored.

In this work, these important problems will be addressed. We first derive the expression for the collision-induced amplitude shift in a fast two-soliton collision described by the coupled NLS equations with the generic Kerr nonlinearity coefficient γ in the presence of cubic loss and quintic loss. Our perturbative technique is extended from the perturbative method for calculating the effects of nonlinear loss on fast collisions of flat-top solitons in Ref. [24] and on fast collisions of two-dimensional solitons in Ref. [25]. More specifically, our perturbative method is based on the calculations for the collision-induced changes in the envelope of solitons and the approximation of the integrals by looking for fast varying terms of the integrand. The current approach allows one to simply establish the collision-induced amplitude shift in a fast two-soliton collision compared to the approaches in Refs. [13,18,19], which were based on the technique describing small perturbations about the ideal NLS soliton derived by Kaup [26]. The expression for the collision-induced amplitude shift above is useful for applications in multiwavelength optical communication systems. In particular, this expression is then used to establish the LV model for deterministic amplitude dynamics of two soliton sequences of Eq. (1). The derivation for the LV model is similar to that in Refs. [13,18]. Based on the stability analysis for the steady states of the LV model, we obtain the conditions on the physical parameters and achieve a proper choice of the linear amplifier gain-loss for the propagation stabilization of the soliton sequences. Our predictions are carried out by the simulations of the corresponding NLS models with varying γ. Furthermore, based on the numerical simulation results, we also look for the optimal value γ for stabilizing the propagation of the soliton sequences of Eq. (1) and discuss the instability of solitons at long-distance propagation.

The rest of the paper is organized as follows. In section II A, the expression for the collision-induced amplitude shift in a fast two-soliton collision with cubic loss and quintic loss for the generic value γ is established. The numerical simulations are then demonstrated in section II B. In section III A, the LV model for the amplitude dynamics of two soliton sequences of model (1) is derived. The stability of the steady states of the LV model is then analyzed to obtain the conditions for stabilizing the propagation of the soliton sequences. The theoretical predictions are demonstrated by the simulations in section III B. Section IV is reserved for the discussion, while section V is reserved for the conclusions.

EFFECTS OF CUBIC LOSS AND QUINTIC LOSS ON A FAST TWO-SOLITON COLLISION

In this section, we derive the expression for the collision-induced amplitude shift in a fast collision of two single solitons in the presence of cubic loss and quintic loss with the generic Kerr nonlinearity coefficient γ. Then, the simulations are demonstrated.

A. Theoretical calculations for the amplitude dynamics

We study fast collisions between two single solitons in nonlinear optical waveguides described by the system of coupled perturbed NLS equations [13–15]:

$$\begin{aligned} &i\partial_z\psi_i+\partial_t^2\psi_i+\gamma\left|\psi_j\right|^2\psi_j+2\gamma\left|\psi_k\right|^2\psi_j= \\ &-i\widetilde{\varepsilon}_3\left|\psi_j\right|^2\psi_j-2i\widetilde{\varepsilon}_3\left|\psi_k\right|^2\psi_j-i\varepsilon_5\left|\psi_j\right|^4\psi_j \\ &-3i\varepsilon_5\left|\psi_k\right|^4\psi_j-6i\varepsilon_5\left|\psi_k\right|^2\left|\psi_j\right|^2\psi_j, \end{aligned} \tag{2}$$

where $\widetilde{\varepsilon}_3$ is the cubic loss coefficient with $0<\widetilde{\varepsilon}_3\square\ 1$. On the right-hand side of Eq. (2), the first and second terms describe the effects of intrapulse and interpulse interactions due to cubic loss. Other terms and coefficients in Eq. (2) are described in Eq. (1).

First, we consider the propagation of a single soliton described by the NLS equation with cubic loss and quintic loss:

$$\begin{aligned} &i\partial_z\psi_j+\partial_t^2\psi_j+\gamma\left|\psi_j\right|^2\psi_j \\ &=-i\widetilde{\varepsilon}_3\left|\psi_j\right|^2\psi_j-i\varepsilon_5\left|\psi_j\right|^4\psi_j. \end{aligned} \tag{3}$$

The optical soliton j is the fundamental solution of the unperturbed NLS equation $i\partial_z\psi_j+\partial_t^2\psi_j+\gamma\left|\psi_j\right|^2\psi_j=0$, where the soliton envelope is given by $\psi_{s,j}(t,z)=\Psi_{s,j}(t,z)\exp\left(i\chi_j\right)$,

$$\Psi_{s,j}(t,z)=\eta_j\mathrm{sech}\left(x_j\right), \tag{4}$$

$x_j=\sqrt{\gamma/2}\eta_j\left(t-y_j-2\beta_j z\right),\chi_j=\alpha_j+\beta_j\left(t-y_j\right)+\left(\eta_j^2-\beta_j^2\right)z$ and parameters η_j, β_j, α_j and y_j are related to the amplitude, frequency, phase, and position, respectively [15]. One can denote by $w*$ the complex conjugate of a complex number w. We now perform the energy balance calculations for Eq. (3) [27]. That is, simplifying $[w*\times\mathrm{Eq.}(3)-\mathrm{Eq.}(3)*\times w]$ and then integrating the resulting equation over z, it implies:

$$\begin{aligned} &\partial_z\int_{-\infty}^{\infty}\left|\psi_j\right|^2dt \\ &=-2\widetilde{\varepsilon}_3\int_{-\infty}^{\infty}\left|\psi_j\right|^4dt-2\varepsilon_5\int_{-\infty}^{\infty}\left|\psi_j\right|^6dt. \end{aligned} \tag{5}$$

One can use the standard adiabatic perturbation theory for the NLS soliton [28], which has been extensively used in previous studies of NLS equations; see, for example, Refs. [13,18,19]. It arrives at the equation for the amplitude dynamics of the single-soliton propagation of Eq. (3):

$$\frac{d\eta_j(z)}{dz}=-\frac{4\widetilde{\varepsilon}_3}{3}\eta_j^3(z)-\frac{16\varepsilon_5}{15}\eta_j^5(z). \tag{6}$$

Next, let us investigate the effects of cubic loss and quintic loss on a fast collision between two single solitons of Eq. (2). We assume $1/\left|\triangle\beta\right|\square\ 1$ where $\triangle\beta=\beta_2-\beta_1$ and assume two solitons are well separated at the initial propagation distance $z=0$ and at the final distance $z=z_f$. Let z_c be the collision distance, i.e., $z_c=\left|y_2(0)-y_1(0)\right|/\left|2\triangle\beta\right|$, and let $[z_c-\triangle z_c,\ z_c+\triangle z_c]$ be the collision length. Thus, $\triangle z_c\square\ 1$ in a fast collision. Based on the perturbative method developed in Refs. [13,18,19], we look for a solution of Eq. (2) in the form:

$$\psi_j(t,z)=\psi_{j0}(t,z)+\phi_j(t,z) \tag{7}$$

where $\psi_{j0}(t,z)=\Psi_{j0}(t,z)\exp\left(i\chi_{j0}\right)$ is the single-soliton propagation solution of Eq. (3), and $\phi_j(t,z)=\Phi_j(t,z)\exp\left(i\chi_{j0}\right)$ represents a small correction to ψ_{j0} due to interpulse interaction. By using the perturbative technique developed in Refs. [24,25], one can obtain the equation for the collision-induced changes in the envelope of soliton 1. More specifically, one can substitute Eq. (7) into the energy balance equation of Eq. (2) and consider the collision effects of the order of nonlinear loss coefficients. By using the standard adiabatic perturbation theory for the NLS soliton [28] and integrating the resulting equation with respect to z over the interval $[z_c-\triangle z_c,\ z_c+\triangle z_c]$, the following is obtained:

$$\begin{aligned} &\int_{z_c-\triangle z_c}^{z_c+\triangle z_c}\partial_z\int_{-\infty}^{\infty}\left|\psi_1\right|^2dtdz= \\ &\int_{z_c-\triangle z_c}^{z_c+\triangle z_c}\partial_z\int_{-\infty}^{\infty}\Psi_{10}^2dtdz-4\widetilde{\varepsilon}_3L_{1,1} \\ &-2\varepsilon_5\sum_{l=1}^{2}b_{2,l}L_{2,l}, \end{aligned} \tag{8}$$

where $L_{1,1}=\int_{z_c-\triangle z_c}^{z_c+\triangle z_c}\int_{-\infty}^{\infty}\Psi_{20}^2\Psi_{10}^2dtdz$,$L_{2,l}=\int_{z_c-\triangle z_c}^{z_c+\triangle z_c}\int_{-\infty}^{\infty}\Psi_{20}^{2l}\Psi_{10}^{2(2-l)+2}dtdz$,$b_{2,1}=6$, and $b_{2,2}=3$. Let $z_c^-=z_c-\triangle z_c$ and $z_c^+=z_c+\triangle z_c$ for the simplicity of the notation. By the definition of ψ_{j0}, one can use the approximation $\psi_1\left(t,z_c^-\right)\sqcup\psi_{10}\left(t,z_c^-\right)$. Simplifying Eq. (8), it implies:

$$\begin{aligned} &\int_{-\infty}^{\infty}\left|\psi_1\left(t,z_c^+\right)\right|^2dt=-2\varepsilon_5\sum_{l=1}^{2}b_{2,l}L_{2,l}+ \\ &\int_{-\infty}^{\infty}\Psi_{10}^2\left(t,\ z_c^+\right)dt-4\widetilde{\varepsilon}_3L_{1,1}. \end{aligned} \tag{9}$$

By the definition of ψ_{j0}, one has $\Psi_{j0}(t,z)=\eta_j(z)\,\mathrm{sech}\left(x_j\right)$, where $\eta_j(z)$ satisfies Eq. (6). Thus, one then obtains

$$\int_{-\infty}^{\infty}\Psi_{j0}^2(t,z)\,dt=2\eta_j(z)\sqrt{2/\gamma}. \tag{10}$$

We note that $\eta_j\left(z_c^-\right)\sqcup\eta_j\left(z_c^+\right)\sqcup\eta_j(z_c)$ in a fast collision. Let $\triangle\eta_1^{(c)}$ be the total collision-induced amplitude shift of soliton 1. One can express $\psi_1\left(t,z_c^+\right)$ in the following manner:

$$\int_{-\infty}^{\infty}\left|\psi_1\left(t,z_c^+\right)\right|dt=2\left[\eta_1(z_c)+\triangle\eta_1^{(c)}\right]\sqrt{2/\gamma}. \tag{11}$$

Substituting Eqs. (10) and (11) into Eq. (9), it yields:

$$\triangle\eta_1^{(c)}=\sqrt{\gamma/2}\left[-2\widetilde{\varepsilon}_3L_{1,1}-\varepsilon_5\sum_{l=1}^{2}b_{2,l}L_{2,l}\right]. \tag{12}$$

One can simplify Eq. (12) by calculating the integrals $L_{1,l}$ and $L_{2,l}$ with $l = 1,2$. For this purpose, one can approximate these integrals by using the similar calculations in Refs.[24,25]. More specifically, one can concentrate on the fast varying terms of $\Psi_{j0}(t,z)$ in $L_{1,l}$ and $L_{2,l}$, i.e., the factors are $v_j = t - y_{j0} - 2\beta_j z$ and can approximate $\Psi_{j0}(t,z)$ by $\bar{\Psi}_{j0}(v_j, z_c)$. Since the integrands of $L_{1,l}$ and $L_{2,l}$ are exponentially small in the pre- and post- collision regions, one can extend the limits of these integrals to $-\infty$ and ∞. By changing the integration variable with $v_j = t - y_{j0} - 2\beta_j z$ and noting that $\int_{-\infty}^{\infty} \bar{\Psi}_j^{2l}(v_j, z_c)\, dv_j = \int_{-\infty}^{\infty} \Psi_j^{2l}(t, z_c)\, dt$, one can obtain

$$L_{1,1} = \frac{1}{2|\triangle\beta|} \int_{-\infty}^{\infty} \Psi_{20}^2(t,z_c)\, dt \int_{-\infty}^{\infty} \Psi_{10}^2(t,z_c)\, dt \tag{13}$$

and

$$L_{2,l} = \frac{1}{2|\triangle\beta|} \int_{-\infty}^{\infty} \Psi_{20}^{2l}(t,z_c)\, dt \times \int_{-\infty}^{\infty} \Psi_{10}^{2(2-l)+2}(t,z_c)\, dt. \tag{14}$$

Substituting Eqs. (13) and (14) into Eq. (12), it arrives at

$$\triangle\eta_1^{(c)} = \frac{4\sqrt{2/\gamma}}{|\triangle\beta|}[-\widetilde{\varepsilon}_3 \eta_1(z_c)\eta_2(z_c) - 2\varepsilon_5 \eta_1^3(z_c)\eta_2(z_c) - \varepsilon_5 \eta_1(z_c)\eta_2^3(z_c)]. \tag{15}$$

Equation (15) describes the collision-induced amplitude shift of soliton 1 in a fast two-soliton collision described by Eq. (2). It is an extension of Eq. (11) in Ref.[18], of Eq. (10) in Ref.[13] and of Eq. (11) in Ref.[19] (for two-soliton collisions with cubic loss and quintic loss). More specifically, the expression of $\triangle\eta_1^{(c)}$ for $\gamma = 2$ was derived in Ref.[18] with cubic loss only ($\varepsilon_5 = 0$), in Ref.[13] with quintic loss only ($\widetilde{\varepsilon}_3 = 0$) and in Ref.[19] with cubic loss and quintic loss (for two-soliton collisions).

B. Numerical simulations

The analytic predictions for the amplitude dynamics of Eqs. (6) and (15) are derived based on a perturbative approximation, which is valid for $\widetilde{\varepsilon}_3 \square 1$, $\varepsilon_5 \square 1$ and $1/|\triangle\beta| \square 1$. Therefore, it is important to carry out the theoretical results by the simulations of the full NLS model. For this purpose, we validate Eqs. (6) and (15) by the simulations of Eqs. (3) and (2) with varying γ, respectively, using the split-step Fourier method with second-order accuracy[4,6]. That is, the errors for the numerically solving Eqs. (3) and (2) are of order $O(h^3)$, where $h = \triangle z$ is a propagation step-size. The initial conditions for the simulations are given by Eq. (4). Additionally, we use the step sizes in t and z as $\triangle t = 0.0588$ and $\triangle z = 0.001$ and use the computational domain as $-500 \le t \le 500$. We note that the predictions of Eqs. (6) and (15) were carried out by simulations of the corresponding NLS model with $\gamma = 2$ for cubic loss only in Ref.[18] and for quintic loss only in Ref.[13].

First, we verify Eq. (6) by implementing the simulations for the single-soliton propagation of Eq. (3) with $\gamma = 1.8$, as an example, for $j = 1$. The other parameters are $\widetilde{\varepsilon}_3 = 0.01$, $\varepsilon_5 = 0.01$, $\eta_1(0) = 1$, $\beta_1(0) = 5$, $y_1(0) = -20$, $\alpha_1(0) = 0$ and the final propagation distance $z_f = 4$. Figure 1 presents the initial soliton profile $|\psi_1(t,0)|$ and the evolution in z of its profile $|\psi_1(t,z)|$ for $0 < z \le z_f$. In addition, the solito amplitude parameters $\eta_1^{(num)}(z_f)$ and $\eta_1^{(th)}(z_f)$ are calculated, where $\eta_1^{(num)}(z)$ is measured by the simulation of Eq. (3), and $\eta_1^{(th)}(z)$ is calculated from Eq. (6). The relative error in measuring $\eta_1(z)$ which is defined by $\left|\eta_1^{(th)}(z) - \eta_1^{(num)}(z)\right| / \eta_1^{(th)}(z)$ is less than 5.5×10^{-4} for $0 < z \le z_f$.

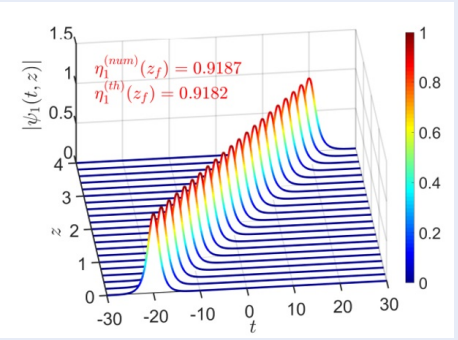

Figure 1: (Color online) The initial soliton profile $|\psi_1(t,0)|$ and its evolution profile $|\psi_1(t,z)|$ for $0 < z \le z_f$ obtained by the simulation of Eq. (3) with $\gamma = 1.8$, $\beta_1(0) = 5$ and $y_1(0) = -20$.

Second, we demonstrate a fast two-soliton collision by the simulation of Eq. (2) with $\gamma = 1.8$. The other parameters are $\widetilde{\varepsilon}_3 = 0.01$, $\varepsilon_5 = 0.01$, $\eta_1(0) = 1$, $\eta_2(0) = 1$, $\beta_1(0) = 0$, $\beta_2(0) = 20$, $y_1(0) = 0$, $y_2(0) = -20$, $\alpha_1(0) = 0$, and $\alpha_2(0) = 0$. Thus, the collision distance is $z_c = 0.5$. Figure 2 depicts the evolution of two soliton profiles over $[0, z_f]$ obtained by the simulation using the contour plot, where $z_f = 2z_c = 1$. In addition, the collision-induced amplitude shifts $\triangle\eta_1^{(c)(num)}$ and $\triangle\eta_1^{(c)(th)}$ are calculated, where $\triangle\eta_1^{(c)(num)}$ is measured by the simulation of Eq. (2), and $\triangle\eta_1^{(c)(th)}$ is calculated from Eq. (15). The relative error in measuring $\triangle\eta_1^{(c)}$, which is defined by $\left|\triangle\eta_1^{(c)(th)} - \triangle\eta_1^{(c)(num)}\right| / \left|\triangle\eta_1^{(c)(th)}\right|$, is 0.02.

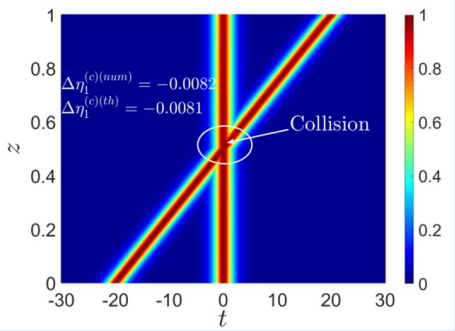

Figure 2: (Color online) The contour plot for soliton profiles over [0, $z_f = 1$] in a fast two-soliton collision at the propagation distance $z_c = 0.5$ obtained by the simulation of Eq. (2) with $\gamma = 1.8$, $\beta_1(0) = 0$, and $\beta_2(0) = 20$.

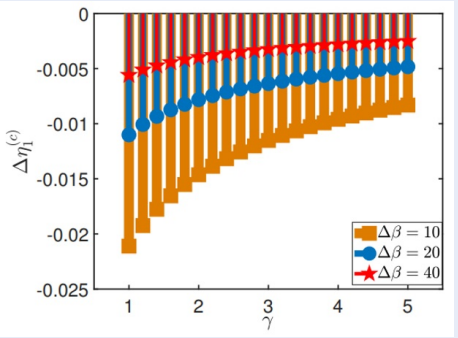

Figure 3: (Color online) The dependence of $\triangle\eta_1^{(c)}$ on γ for each $\triangle\beta$. The orange-squared, blue-circled, and red-stared stems represent $\triangle\eta_1^{(c)}$ measured by the simulations of Eq. (2) with $\triangle\beta = 10$, $\triangle\beta = 20$, and $\triangle\beta = 40$, respectively.

Finally, we study the contribution of the Kerr nonlinearity coefficient γ to $\triangle\eta_1^{(c)}$ and study the dependence of $\triangle\eta_1^{(c)}$ on $\triangle\beta$. For this purpose, we implement the simulations for Eq. (2) with varying γ as $1 \leq \gamma \leq 5$ and varying $\triangle\beta$ as $10 \leq \triangle\beta \leq 60$ as a concrete example. We use the parameters $\widetilde{\varepsilon}_3 = 0.01$, $\varepsilon_5 = 0.01$, $\eta_1(0) = 1$, $\eta_2(0) = 1$, $\beta_1(0) = 0$, $y_1(0) = 0$, $y_2(0) = -20$, $\alpha_1(0) = 0$, $\alpha_2(0) = 0$ and $z_f = 2z_c$. We observe very good agreement between the simulation results and the theoretical predictions of $\triangle\eta_1^{(c)}$. In fact, the results are summarized as follows:

- For $1 \leq \gamma \leq 2.6$: The relative error in measuring $\triangle\eta_1^{(c)}$ is less than 0.03 for $10 \leq \triangle\beta \leq 60$.
- For $2.6 < \gamma \leq 3.2$: The relative error in measuring $\triangle\eta_1^{(c)}$ is less than 0.025 for $12 \leq \triangle\beta \leq 60$ and less than 0.05 for $10 \leq \triangle\beta < 12$.
- For $3.2 < \gamma \leq 4$: The relative error in measuring $\triangle\eta_1^{(c)}$ is less than 0.045 for $12 \leq \triangle\beta \leq 60$ and less than 0.08 for $10 \leq \triangle\beta < 12$.
- For $4 < \gamma \leq 5$: The relative error in measuring $\triangle\eta_1^{(c)}$ is less than 0.03 for $15 \leq \gamma \leq 60$, less than 0.07 for $12 \leq \triangle\beta < 15$, and less than 0.11 for $10 \leq \triangle\beta < 12$.

Overall, the relative error in measuring $\triangle\eta_1^{(c)}$ is less than 0.045 for $12 \leq \triangle\beta \leq 60$, i.e., for fast collisions, with $1 \leq \gamma \leq 4$. The simulation results for $\triangle\eta_1^{(c)}$ are presented in Figure 3 with $\triangle\beta = 10,\ 20,\ 40$ for $1 \leq \gamma \leq 5$.

In summary, the simulation results above validate the theoretical predictions for $\triangle\eta_1^{(c)}$ in Eq. (15).

CROSS-TALK DYNAMICS IN A TWO-CHANNEL WAVEGUIDE SYSTEM

In this section, we establish a reduced model for the deterministic amplitude dynamics of two soliton sequences with linear gain-loss, GL gain-loss profile, and Kerr nonlinearity with the generic Kerr nonlinearity coefficient γ. Then, the simulations are demonstrated. Furthermore, we look for the optimal value γ for stabilization of the propagation of soliton sequences.

A. A Lotka-Volterra model for the amplitude dynamics

We consider the transmission of two soliton sequences in the waveguide system described by Eq. (1). In this paper, we consider the form of $\widehat{g}_j(\omega)$ as follows:

$$\widehat{g}_j(\omega) = \begin{cases} g_j, \text{ if } \beta_j(0)/2 - W/2 < \omega < \beta_j(0)/2 + W/2 \\ g_L, \text{ elsewhere.} \end{cases} \quad (16)$$

In Eq. (16), g_j is the constant net linear gain or loss for the jth sequence, which is determined by the difference between the linear amplifier gain and linear waveguide loss, $g_L < 0$ is the loss required for suppressing the radiation emission, and the spectral width W satisfies $1\square\ W \leq \triangle\beta$ with $\triangle\beta = |\beta_2(0) - \beta_1(0)|$. The values of g_L and W are determined by simulations of Eqs. (1) and (16) such that one can yield the longest stable propagation distance. We emphasize that similar forms of $\widehat{g}_j(\omega)$, which are the step gain-loss functions, have been studied in

Refs. [22,23]. In addition, further applications of the step gain-loss functions have been studied in Refs. [15,21].

The derivation of the LV model for deterministic amplitude dynamics of two soliton sequences of Eqs. (1) and (16) is similar to the one carried out in Ref. [13] for γ = 2. It is based on the following assumptions. (1) The temporal separation T between adjacent solitons in each sequence is $T\square$ 1 In addition, the amplitudes are equal for all solitons from the same sequence, but they cannot be equal for solitons from different sequences. (2) Since $T\square$ 1, the solitons in each sequence are well separated. Thus, the intrasequence interaction is exponentially small and is neglected. (3) The two soliton sequences circulate in a waveguide loop with $\triangle\beta\square$ 1. (4) The gain-loss is assumed to be a weak perturbation. As a result, high-order effects due to collision-induced frequency shifts and the emission of radiation are neglected.

Since the sequences of solitons are periodic, the amplitudes of all solitons in a given sequence undergo the same dynamic evolution. We take into account the single pulse amplitude shift, which is given by Eq. (6), and the collision-induced amplitude shift, which is given by Eq. (15). Using similar calculations for deriving the LV model in Ref. [13] leads to the equation for the amplitude dynamics of the jth soliton sequence:

$$\frac{d\eta_j}{dz} = \eta_j[g_j + \frac{4\varepsilon_3}{3}\eta_j^2 - \frac{16\varepsilon_5}{15}\eta_j^4 + \frac{8\sqrt{2/\gamma}}{T}\varepsilon_3\eta_k - \frac{8\sqrt{2/\gamma}}{T}\varepsilon_5\eta_k\left(2\eta_j^2+\eta_k^2\right). \quad (17)$$

In multichannel waveguide systems, it is usually desired to achieve a steady state in which the amplitudes of solitons in all sequences are equal and constant [4]. Therefore, one can look for an equilibrium state of Eq. (17) in the form $\eta_1^{(eq)} = \eta_2^{(eq)} = \eta > 0$. Setting the right-hand sides of Eq. (17) equal to zero and letting $\kappa = \varepsilon_3/\varepsilon_5$, it arrives at

$$g_j = 4\varepsilon_5\eta\left(-\frac{\kappa}{3}\eta + \frac{4}{15}\eta^3 - \frac{2\kappa\sqrt{2/\gamma}}{T} + \frac{6\sqrt{2/\gamma}}{T}\eta^2\right). \quad (18)$$

Substituting Eq. (18) into Eq. (17), one can obtain a simpler form of the LV model for analysis and numerical simulations:

$$\frac{d\eta_j}{dz} = \varepsilon_5\eta_j\{\frac{4\kappa}{3}\left(\eta_j^2-\eta^2\right) - \frac{16}{15}\left(\eta_j^4-\eta^4\right) + \frac{8\kappa\sqrt{2/\gamma}}{T}(\eta_k-\eta) - \frac{8\sqrt{2/\gamma}}{T}\left[\eta_k\left(2\eta_j^2+\eta_k^2\right)-3\eta^2\right]\}. \quad (19)$$

Equation (19) describes the amplitude dynamics of solitons in a two-channel waveguide system with the generic Kerr nonlinearity coefficient γ and with the linear gain-loss and GL gain-loss profiles. For γ = 2, Eq. (19) becomes Eq. (25) in Ref. [13], Eq. (4) in Ref. [14], and Eq. (5) in Ref. [16]. From Eq. (19), one can see that (η,η) and $(0,0)$ are the equilibrium states of the model for any positive values of η, κ, and T.

We now investigate the predictions of the LV model (19) for the transmission stabilization of two soliton sequences. As a concrete example, one can choose $\eta = 1$. We require that the equilibrium point at $(1,1)$ is stable so that the soliton amplitude values of the two sequences approach 1 as the propagation distance increases. Furthermore, we also require that the equilibrium point at $(0,0)$ is stable. This requirement is important for suppressing radiative instability due to the growth of small amplitude waves. In addition, by the simulations, one can define $0.9 \le \gamma \le 5.4$ for the propagation stabilization of soliton sequences. From the above requirements and noting that $T\square$ 1, the linear stability analysis implies the following conditions on T and κ:

$$\frac{2\left(2T\sqrt{\gamma}+45\sqrt{2}\right)}{5\left(T\sqrt{\gamma}+6\sqrt{2}\right)} < \kappa < \frac{2\left(4T\sqrt{2\gamma}-15\right)}{5\left(T\sqrt{2\gamma}-6\right)}. \quad (20)$$

When γ = 2, condition (20) becomes condition (27) in Ref. [13].

Overall, the LV model (19) is an extension of the one in Ref. [13], where the reduced model for deterministic amplitude dynamics of two soliton sequences was derived with γ = 2. The LV model (19) with γ = 2 was also used in Refs. [14,16] for studying the robust transmission stabilization and dynamic switching of two soliton sequences.

B. Numerical simulations

The derivation of the LV model (19) is based on several simplifying assumptions. In particular, Eq. (19) provides an approximate description for the amplitude dynamics of the two soliton sequences of Eq. (1) while neglecting the effects of the radiation emission, pulse distortion, and intrasequence interaction. This might breakdown the predictions of the LV model at large propagation distances. Therefore, it is necessary to carry out the predictions of the LV model (19) by simulations with the full coupled-NLS model (1). In particular, we will address the important question about the optimal value γ for stabilization of the propagation of soliton sequences described by Eq. (1).

The NLS model (1) is numerically solved by using the split-step Fourier method with periodic boundary conditions with second-order accuracy [4,6]. The usage of periodic boundary conditions means that the

simulations are implemented in a closed waveguide loop. The initial conditions for the simulations are in the form of two periodic sequences of $2J+1$ solitons with amplitudes $\eta_j(0)$, frequencies $\beta_j(0)$, positions δ_j, and zero phases as follows:

$$\psi_j(t,0) = \sum_{l=-J}^{J} \frac{\eta_j(0)\exp\left[i\beta_j(0)\left(t-lT-\delta_j\right)\right]}{\cosh\left[\eta_j(0)\left(t-lT-\delta_j\right)\right]} \quad (21)$$

where $j=1,2$.

As a concrete example, we present the simulation results with varying γ as $0.9 \le \gamma \le 5.4$ and with parameters used in Ref.[14] as $T=20,\ \varepsilon_5=0.01,\ \kappa=1.5,\ \beta_1(0)=0$ and $\beta_2(0)=40$. These parameters satisfy Eq. (20). Additionally, we use $J=1,\ \delta_1=0$ and $\delta_2=T/2$. In addition, we use the step sizes in t and z as $\triangle t=0.0588$ and $\triangle z=0.001$ and use the computational domain as $-30 \le t \le 30$. The simulations are implemented up to a distance z_s, where z_s is the distance at which the instability appears. More specifically, we define z_s as the largest distance at which $I_j(z) < C$, see Ref.[23], where

$$I_j(z) = \frac{\left|\left|\left|\psi_j^{(th)}(t,z)\right| - \left|\psi_j^{(num)}(t,z)\right|\right|\right|}{\left|\left|\psi_j^{(th)}(t,z)\right|\right|}, \quad (22)$$

$||\psi_j|| = \left[\int_{t_{min}}^{t_{max}} |\psi_j|^2\, dt\right]^{1/2}$, $t_{min} = -t_{max} = -30$, and C is a constant. In practice, we use $C=0.05$ and note that this value of C was used in Ref.[23] for studying the transmission stabilization of soliton sequences. We also note that the predictions of Eq. (19) with $\gamma=2$ were carried out by the simulations in Ref.[13] and were used in Refs.[14,16] for studying the transmission stabilization and on-off switching of soliton sequences.

First, we illustrate the evolution of the two soliton sequences of Eq. (1) with $\widehat{g}_j(\omega)$ in Eq. (16). The initial amplitude parameters are $\eta_1(0)=\eta_2(0)=1$. The profiles of two soliton sequences over $[0,\ z_f]$, where $z_f=0.5$, are presented in Figure 4 using the contour plot. One can measure the net linear loss g_j in Eq. (16) as $g_1=g_2=-0.003009$ and the amplitudes of soliton sequences as $\eta_1(z)=\eta_2(z)=1$ for $z\in[0,\ z_f]$.

Second, we carry out the predictions of Eq. (19) by the simulations of Eqs. (1) and (16). The parameters are $\eta_1(0)=1.1,\ \eta_2(0)=0.9, \gamma=1.8,\ \varepsilon_5=0.01$ and $W=15$. We use $C=0.05$ to define z_s. The simulation results are presented in Figure 5. Figure 5(a) shows the dependence of $\eta_j(z)$ on z for $z\in[0,z_s]$, where $z_s=28890$, while Figure 5(b) presents $\eta_j(z)$ at short distances. The profiles of two soliton sequences $|\psi_j(t,z)|$ are shown in Figure 5(c) at $z=z_s$

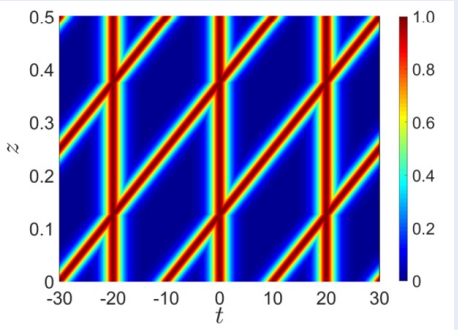

Figure 4: (Color online) An illustration of the evolution of two soliton sequences of Eqs. (1) and (16) over $[0,\ z_f=0.5]$ using the contour plot. The collisions of two soliton sequences occur at the propagation distances $z=0.125$ and $z=0.375$.

and in Figure 5(d) at $z=z_f$ with $z_f=30000>z_s$. As seen in Figures 5(a) and (b), the soliton amplitudes tend to the equilibrium value $\eta=1$ with increasing distance, i.e., the transmission is stable up to the distance $z=z_s$. One can observe the very good agreement for $\eta_j(z)$ between the predictions of the LV model (19) and the simulation of the coupled NLS model (1) for $0<z\le z_s$. In addition, as seen in Figure 5(c), the agreement for the soliton profiles obtained by the simulation at $z=z_s$ and its theoretical prediction is good, i.e., the solitons retain the shape at $z=z_s$. For $z>z_s$, the transmission of solitons is unstable. As seen in Figure 5(d), the agreement for the soliton profiles obtained by the simulation and the theoretical prediction is good for sequence 1 but it is not good for sequence 2 due to the intrasequence effect. More specifically, one can observe the difference between the simulation result and the theoretical prediction for the position of the 1st soliton and of the 2nd soliton of sequence 2. Moreover, by implementing the simulations with $8\le W\le 45$, one can observe very good agreement between the simulation results and the theoretical predictions for the soliton amplitudes $\eta_j(z)$ and for the soliton profiles $|\psi_j(t,z)|$ for $0<z\le z_s$. Additionally, one can obtain the optimal value W for the transmission stabilization of two soliton sequences in the interval $[10,\ 25]$. As an example, one obtains z_s of 13880, 28890, 14070, 12870, 2070, 2080, 2100, and 2080 for W as 10, 15, 20, 25, 30, 35, 40, and 45, respectively.

Third, we validate the predictions of Eq. (19) by the simulations of Eqs. (1) and (16) with varying γ and with varying ε_5. The parameters are $\eta_1(0)=1.1,\ \eta_2(0)=0.9$ and $W=15$. The simulations are implemented up to a short distance such that one can

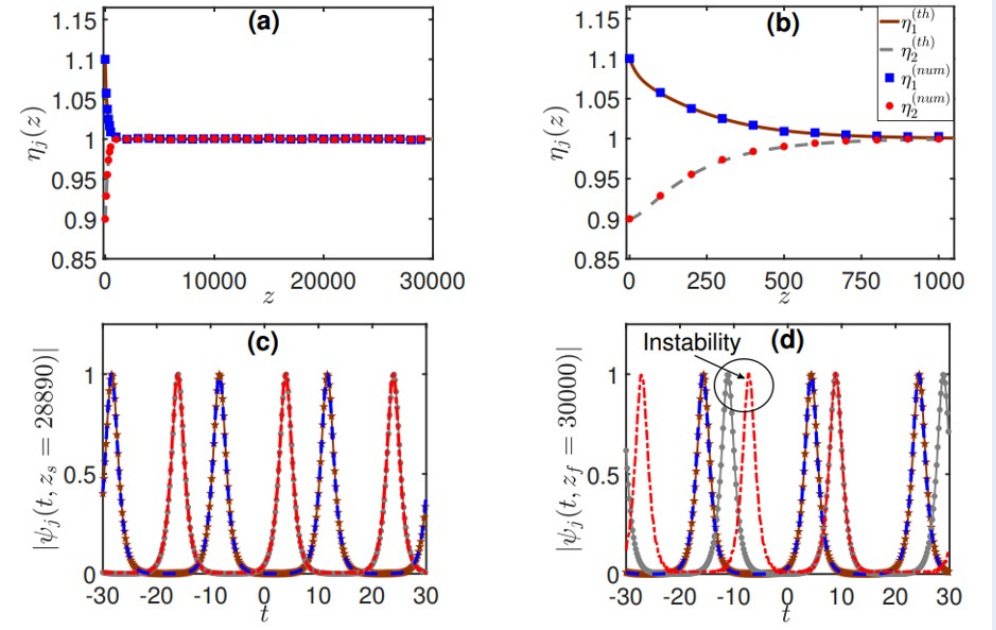

Figure 5: (Color online) The simulation results for Eqs. (1) and (16) with $\gamma = 1.8$, $\varepsilon_5 = 0.01$, and $W = 15$. (a) Dependence of $\eta_j(z)$ on z for $0 < z \leq z_s$. (b) The magnified version of $\eta_j(z)$ in (a) at a short distance. The brown solid and gray dashed curves represent $\eta_1(z)$ and $\eta_2(z)$, respectively, obtained by the theoretical predictions of Eq. (19). The blue squares and red circles correspond to $\eta_1(z)$ and $\eta_2(z)$, respectively, measured by the simulation. (c - d) The soliton profiles at $z = z_s$ (c) and at $z = z_f$ (d). The blue dashed and red dashed-dotted curves represent $|\psi_1(t,z)|$ and $|\psi_2(t,z)|$, respectively, obtained by the simulation. The brown solid-starred and gray solid curves correspond to the theoretical predictions for $|\psi_1(t,z)|$ and $|\psi_2(t,z)|$, respectively.

clearly observe the approach of the soliton amplitudes $\eta_j(z)$ to the equilibrium value $\eta = 1$. For example, we use $z_f = 1000$. Figure 6 (a) depicts $\eta_1(z)$ for $0 < z \leq z_f$ with $\varepsilon_5 = 0.01$ and with $\gamma = 1$, $\gamma = 2.2$, and $\gamma = 4$, while Figure 6 (b) shows $\eta_1(z)$ for $0 < z \leq z_f$ with $\varepsilon_5 = 0.01,\ 0.02,\ 0.03,\ 0.05$ and $\gamma = 1.8$. The soliton amplitude $\eta_1(z)$ tends to the equilibrium value $\eta = 1$ with increasing distance. Additionally, the agreement for $\eta_1(z)$ between the predictions of the LV model (19) and the simulation results of the coupled NLS model (1) for $0 < z \leq z_f$ is very good. In addition, as seen in Figure 6(b), the approach of the soliton amplitude $\eta_1(z)$ to $\eta = 1$ is faster as ε_5 increases. This observation is similar to the one in Ref.[14] for $\gamma = 2$.

Finally, we investigate the use of the frequency dependent linear-gain loss for enhancing the transmission stabilization at long distances compared to the use of the constant gain-loss coefficients. Furthermore, we address the important question about the optimal value γ for stabilization of the propagation of soliton sequences described by Eq. (1). For this purpose, we implement the simulations for Eq. (1) with $\widehat{g}_j(\omega) = g_j = \text{const}$ and with $\widehat{g}_j(\omega)$ of Eq. (16) for varying γ as $0.9 \leq \gamma \leq 5.4$. The initial amplitude parameters are $\eta_1(0) = 1.1$ and $\eta_2(0) = 0.9$. Additionally, we use $W = 15$ and $W = 20$. In addition, we use $C = 0.05$ to define z_s. The simulations are implemented up to $z_f > z_s$ such that the instability of the solitons can be clearly observed. The simulation results for z_s are shown in Figure 7. The values of z_s obtained by the simulations of Eq. (1) using the frequency-dependent gain-loss $\widehat{g}_j(\omega)$ in Eq. (16) are significantly larger than those obtained by using constant gain-loss coefficients. These observations are the same as those in Ref.[23] for studying the propagation of solitons with delayed Raman response. Furthermore, as seen in Figure 7, the optimal value γ for the transmission stabilization of two soliton sequences can be found in the interval [1.6, 2.6]. In particular, one can yield the longest stable propagation distance for two soliton sequences with $\gamma = 1.8$. More specifically, with $W = 15$, one can observe that $z_s = 28890$ for $\gamma = 1.8$ is larger than z_s for other values of γ. In addition, one can observe the profiles of the soliton sequences at $z = z_f > z_s$ in Table 1 and in Figure 8. Let us describe the results of Table 1 as follows. For example, the second row of Table 1 with №1 describes the simulation results with $\gamma \in [0.9, 1.6]$. For these val-

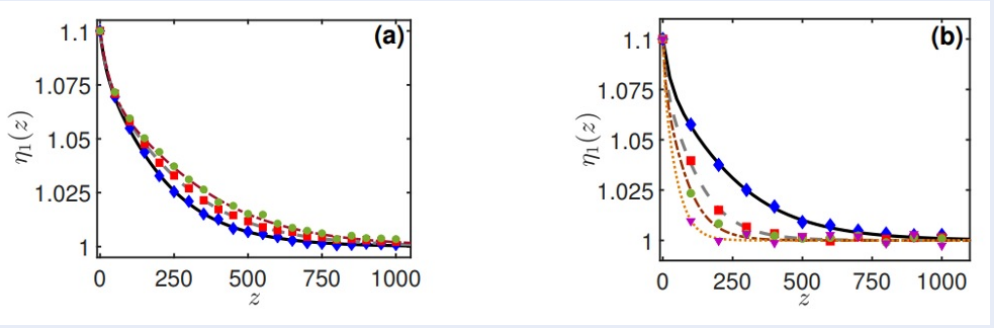

Figure 6: (Color online) Dependence of $\eta_1(z)$ on z obtained by simulations of Eqs. (1) and (16) with varying γ and varying ε_5. (a) The simulation results with $\varepsilon_5 = 0.01$ and varying γ as $\gamma = 1$, $\gamma = 2.2$, and $\gamma = 4$. The black solid, gray dashed, and brown dashed-dotted curves represent $\eta_1(z)$ obtained by the theoretical predictions of Eq. (19) for $\gamma = 1$, $\gamma = 2.2$, and $\gamma = 4$, respectively. The blue diamonds, red squares, and green circles correspond to $\eta_1(z)$ measured by the simulations for $\gamma = 1$, $\gamma = 2.2$, and $\gamma = 4$, respectively. (b) The simulation results with $\gamma = 1.8$ and varying ε_5 as 0.01, 0.02, 0.03, and 0.05. The black solid, gray dashed, brown dashed-dotted, and orange dotted curves represent $\eta_1(z)$ obtained by the theoretical predictions of Eq. (19) with $\varepsilon_5 = 0.01$, 0.02, 0.03, and 0.05, respectively. The blue diamonds, red squares, green circles, and purple triangles correspond to $\eta_1(z)$ measured by the simulations with $\varepsilon_5 = 0.01$, 0.02, 0.03, and 0.05, respectively.

ues γ, one can observe the distortion of the bottom of soliton sequences 1 and 2 at $z = z_f$, while the intrasequence effects at $z = z_f$ are not observed. The profiles of soliton sequences are presented in Figures 8 (a) and (b) for $\gamma = 1.4 \in [0.9, 1.6]$. Similar results are obtained for other values of ε_5. That is, one can find that the optimal value γ for the transmission stabilization of two soliton sequences is in the interval [1.6, 2.6]. For example, one can yield the longest stable propagation distance for two soliton sequences with $\gamma = 1.8$ as $z_s = 17080$ for $\varepsilon_5 = 0.02$ and $z_s = 12590$ for $\varepsilon_5 = 0.03$.

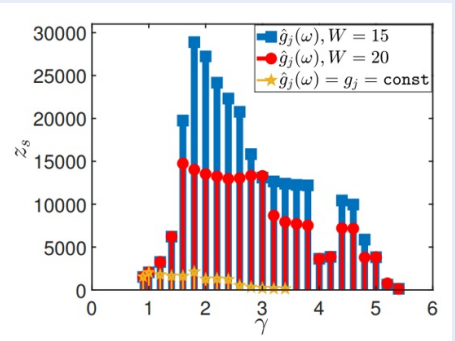

Figure 7: (Color online) Dependence of the stable propagation distance z_s on γ obtained by the simulations of Eq. (1). The value z_s is defined by using Eq. (22) and C = 0.05. The yellow-stared stems represent z_s obtained by simulations with $\hat{g}_j(\omega) = g_j$ = constant. The red-circled and blue squared stems correspond to z_s obtained by simulations with $\hat{g}_j(\omega)$ of Eq. (16) for $W = 20$ and $W = 15$, respectively.

In summary, the agreement between the simulation results and the theoretical predictions for the soliton amplitudes $\eta_j(z)$ and for the soliton profiles $|\psi_j(t,z)|$ is good for $0 < z \leq z_s$. This validates the theoretical prediction for the LV model (19).

DISCUSSION

We derived the expression for the collision-induced amplitude dynamics in a fast collision of two single solitons propagating in nonlinear optical waveguides with the generic Kerr nonlinearity coefficient γ, weak cubic loss, and weak quintic loss. Our perturbative technique is extended from the perturbative technique for calculating the effects of nonlinear loss on fast collisions of flat-top solitons in Ref.[24] and on fast collisions of two-dimensional solitons in Ref.[25]. The current expression for the collision-induced amplitude dynamics is a modification of the one in Ref.[13], which was derived by a different approach. Furthermore, this expression was then used to investigate the amplitude dynamics of soliton sequences in multi-wavelength optical communication systems. Particularly, we used the collision-induced amplitude dynamics above to derive the LV model for deterministic amplitude dynamics of two soliton sequences in Kerr media with the generic Kerr nonlinearity coefficient γ, the frequency dependent linear gain-loss, and the GL gain-loss profile. The derivation for the LV model is similar to that in Refs.[13,18]. We then analyzed the stability analysis for the steady states of the LV model to obtain the conditions on the physical parameters and to achieve a proper choice of the linear amplifier

Table 1: The soliton sequence profiles at $z = z_f$ obtained by simulations of Eqs. (1) and (16) with W = 15

№1	γ	The instability of the soliton profiles		Figures
		The distortion of solitons	The intrasequence effects	
1	[0.9, 1.6]	Yes (for solitons 1 and 2)	No	8(a, b), γ =1.4
2	(1.6, 2.6]	No	Yes (for soliton 2)	5(c, d), γ =1.8
3	(2.6, 2.8]	Yes (for soliton 2)	Yes (for soliton 1)	8(c, d), γ =2.8
4	(2.8, 3.8]	Yes (for soliton 2)	No	8(e, f), γ =3.2
5	(3.8, 4.2]	Yes (for soliton 2)	No	
6	(4.2, 4.6]	No	Yes (for soliton 2)	
7	(4.6, 5.4]	Yes (for soliton 2)	Yes (for soliton 2)	

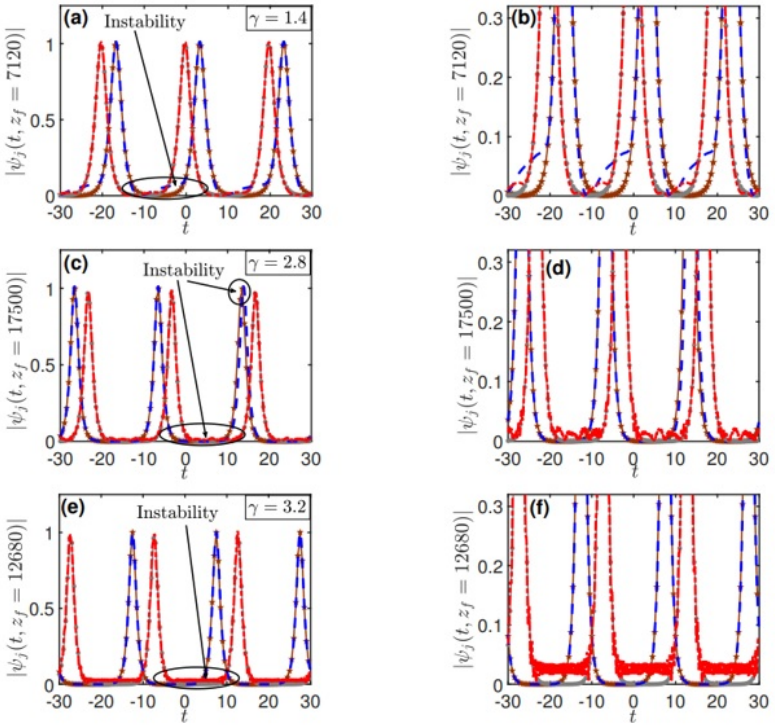

Figure 8: (Color online) The soliton profiles at $z = z_f$ obtained by the simulations of Eqs. (1) and (16) with W = 15 and their theoretical predictions for γ = 1.4 (a), γ = 2.8 (c), and γ = 3.2 (e). (b, d, f) Magnified versions of graphs in (a, c, e), respectively, for small values of $|\psi_j(t, z_f)|$.The symbols are the same as those in Figure 5(c) and (d).

gain-loss for the propagation stabilization of the soliton sequences.

Our theoretical calculations were confirmed by numerical simulations of the corresponding NLS models with varying γ. In addition, we also determined the optimal value γ for stabilizing the propagation of the soliton sequences of Eq. (1) and discussed the instability of solitons at long-distance propagation. One can expect that the current perturbation method, which was used to investigate the collision-induced amplitude dynamics of two solitons with nonlinear loss, can be applied to study the soliton dynamics with delayed Raman response or with other dissipative perturbations for the generic Kerr nonlinearity coefficient in a similar manner. Furthermore, the study for the LV model and the investigation for the optimal value γ with the frequency dependent linear gain-loss in the current paper can be used to study the

on-off switching of solitons in multichannel optical waveguide systems, which has been only explored in several earlier works for $\gamma = 2$, such as in Refs. [14,16,22].

CONCLUSIONS

In this paper, we investigated the soliton dynamics in optical waveguides with the generic Kerr nonlinearity coefficient γ and nonlinear gain-loss. The collision-induced amplitude dynamics of two solitons in the presence of weak cubic loss and weak quintic loss are derived for the generic coefficient γ for the first time. Furthermore, the robustness of the use of the frequency-dependent linear gain-loss for stabilizing the propagation of soliton sequences in the presence of the GL gain loss profile with the generic coefficient γ was studied. In addition, the optimal value of the Kerr nonlinearity coefficient for the propagation stabilization of soliton sequences in the broadband optical waveguide system with a GL gain-loss profile was addressed.

LIST OF ABBREVIATIONS

GL Ginzburg-Landau
LV Lotka-Volterra
NLS Nonlinear Schrödinger
WDM Wavelength-division-multiplexing

COMPETING INTERESTS

The authors declare that they have no conflicts of interest.

ACKNOWLEDGMENTS

This work is funded by the Vietnam National Foundation for Science and Technology Development (NAFOSTED) under Grant No. 107.99-2019.340. We thank Dr. Quan M. Nguyen for his meaningful discussions on the paper.

REFERENCES

1. Ablowitz MJ. Nonlinear Dispersive Waves: Asymptotic Analysis and Solitons. Cambridge University Press. 2011;.
2. Tao T. Nonlinear dispersive equations: Local and global analysis, in: Proceedings of the CBMS Regional Conference Series in Mathematics, 106, AMS. 2006;Available from: https://doi.org/10.1090/cbms/106.
3. Kartashov YV, Malomed BA, Torner L. Solitons in nonlinear lattices. Rev Mod Phys. 2011;83:247;Available from: https://doi.org/10.1103/RevModPhys.83.247.
4. Agrawal GP. Nonlinear Fiber Optics. Academic, San Diego, CA. 2019;.
5. Mollenauer LF, Gordon JP. Solitons in Optical Fibers: Fundamentals and Applications, Academic, San Diego, CA. 2006;.
6. Yang J. Nonlinear Waves in Integrable and Nonintegrable Systems. SIAM, Philadelphia. 2010;.
7. Cisneros-Ake LA, Carretero-González R, Kevrekidis PG, Malomed BA. Dynamics and stabilization of bright soliton stripes in the hyperbolic-dispersion nonlinear Schrödinger equation. Commun Nonlinear Sci Numer Simulat. 2019;74:268-281;Available from: https://doi.org/10.1016/j.cnsns.2019.03.012.
8. Essiambre R-J, Kramer G, Winzer PJ, Foschini GJ, Goebel B. Capacity limits of optical fiber networks. J Lightwave Technol. 2010;28:662;Available from: https://doi.org/10.1109/JLT.2009.2039464.
9. Lin Q, Painter OJ, Agrawal GP. Nonlinear optical phenomena in silicon waveguides: Modeling and applications. Opt Express. 2007;15:16604;Available from: https://doi.org/10.1364/OE.15.016604.
10. Foster MA, Turner AC, Lipson M, Gaeta AL. Nonlinear optics in photonic nanowires. Opt Express. 2008;16:1300;Available from: https://doi.org/10.1364/OE.16.001300.
11. Zhang H, Tang DY, Wu X, Zhao LM. Multiwavelength dissipative soliton operation of an erbium-doped fiber laser. Opt Express. 2009;17:12692;Available from: https://doi.org/10.1364/OE.17.012692.
12. Liu X, Han D, Sun ZP, Zeng C, Lu H, Mao D, Cui Y, Wang F. Versatile multiwavelength ultrafast fiber laser mode-locked by carbon nanotubes. Sci Rep. 2013;3:2718;Available from: https://doi.org/10.1038/srep02718.
13. Peleg A, Chung Y. Cross-talk dynamics of optical solitons in multichannel waveguide systems with a Ginzburg-Landau gain-loss profile. Phys Rev A. 2012;85:063828;Available from: https://doi.org/10.1103/PhysRevA.85.063828.
14. Chakraborty D, Peleg A, Jae-Hun Jung. Stable long-distance propagation and on-off switching of colliding soliton sequences with dissipative interaction. Phys Rev A. 2013;88:023845;Available from: https://doi.org/10.1103/PhysRevA.88.023845.
15. Chakraborty D, Peleg A, Nguyen QM. Stabilizing soliton-based multichannel transmission with frequency dependent linear gain-loss. Opt Commun. 2016;371:252-262;Available from: https://doi.org/10.1016/j.optcom.2016.03.039.
16. Nguyen QM, Peleg A, Tran TP. Robust transmission stabilization and dynamic switching in broadband hybrid waveguide systems with nonlinear gain and loss. Phys Rev A. 2015;91:013839;Available from: https://doi.org/10.1103/PhysRevA.91.013839.
17. The dimensionless distance z in Eq. (1) is $z = X/(2L_D)$, where X is the dimensional distance, $L_D = \tau_0^2/|\tilde{\beta}_2|$ is the dimensional dispersion length, τ_0 is the soliton width, and $\tilde{\beta}_2$ is the second-order dispersion coefficient. The dimensionless time is $t = \tau/t_0$, where τ is the time. The dimensionless electric field is $\psi = E/\sqrt{P_0}$, where E is proportional to the electric field and P_0 is the peak power. The dimensionless second-order dispersion coefficient is $d = -1 = \tilde{\beta}_2/(\gamma P_0 \tau_0^2)$. The coefficients ε_3 and ε_5 are related to the dimensional cubic gain ρ_3 and quintic loss ρ_5, by $\varepsilon_3 = 2\rho_3/\gamma$ and $\varepsilon_5 = 2\rho_5 P_0/\gamma$, respectively. The dimensionless linear gain-loss $\hat{g}$ is related to the dimensional $\tilde{g}$ by $\hat{g} = 2\tau_0^2 \tilde{g}/|\tilde{\beta}_2|$.

18. Peleg A, Nguyen QM, Chung Y. Cross-talk dynamics of optical solitons in a broadband Kerr nonlinear system with weak cubic loss. Phys Rev A. 2010;82:053830;Available from: https://doi.org/10.1103/PhysRevA.82.053830.
19. Peleg A, Nguyen QM, Glenn P. Many-body interaction in fast soliton collisions. Phys Rev E. 2014;89:043201 ;Available from: https://doi.org/10.1103/PhysRevE.89.043201.
20. Boyd RW. Nonlinear Optics. Academic, San Diego, CA. 2008;.
21. Nguyen QM, Huynh TT. Frequency shifting for solitons based on transformations in the Fourier domain and applications. Appl Math Model. 2019;72:306-323;Available from: https://doi.org/10.1016/j.apm.2019.03.019.
22. Peleg A, Nguyen QM, Huynh TT. Stable scalable control of soliton propagation in broadband nonlinear optical waveguides. Eur Phys J D. 2017;71:30;Available from: https://doi.org/10.1140/epjd/e2016-70387-x.
23. Peleg A, Nguyen QM, Tran TP. Transmission stability and Raman-induced amplitude dynamics in multichannel soliton-based optical waveguide systems. Opt Commun. 2016;380:41-56;Available from: https://doi.org/10.1016/j.optcom.2016.05.061.
24. Huynh TT, Nguyen QM. Fast soliton interactions in cubic-quintic nonlinear media with weak dissipation. Appl Math Model. 2021;97:650-665;Available from: https://doi.org/10.1016/j.apm.2021.04.022.
25. Nguyen QM, Huynh TT. Collision-induced amplitude dynamics of fast 2D solitons in saturable nonlinear media with weak nonlinear loss. Nonlinear Dyn. 2021;104:4339-4353;Available from: https://doi.org/10.1007/s11071-021-06548-3.
26. Kaup DJ. Perturbation theory for solitons in optical fibers. Phys Rev A. 1990;42:5689;Available from: https://doi.org/10.1103/PhysRevA.42.5689.
27. Debnath L. Nonlinear Partial Differential Equations for Scientists and Engineers. Springer, USA. 2005;.
28. Hasegawa A, Kodama Y. Solitons in Optical Communications. Oxford: Clarendon. 1995;.

Tạp chí Phát triển Khoa học và Công nghệ
Đại học Quốc gia Tp. Hồ Chí Minh

Tạp chí Phát triển Khoa học và Công nghệ
ISSN: 1859-0128
Hình thức xuất bản: In và trực tuyến
Hình thức truy cập: Truy cập mở (Open Access)
Ngôn ngữ bài báo: Tiếng Anh
Tỉ lệ chấp nhận đăng 2021: 72%
Phí xuất bản: Miễn phí
Thời gian phản biện: 43 ngày
Lập chỉ mục (Indexed): Google Scholar, Scilit

SCAN ME

Tạp chí Phát triển Khoa học và Công nghệ - Khoa học Tự nhiên
ISSN: 2588-106X
Hình thức xuất bản: In & trực tuyến
Hình thức truy cập: Truy cập mở
Ngôn ngữ bài báo: Tiếng Việt
Tỉ lệ chấp nhận đăng 2021: 75%
Phí xuất bản: Miễn phí
Thời gian phản biện: 30-45 ngày
Lập chỉ mục (Indexed): Google Scholar, Scilit

SCAN ME

Tạp chí Phát triển Khoa học và Công nghệ - Kĩ thuật và Công nghệ
ISSN: 2615-9872
Hình thức xuất bản: In & trực tuyến
Hình thức truy cập: Truy cập mở
Ngôn ngữ bài báo: Tiếng Việt
Tỉ lệ chấp nhận đăng 2021: 61%
Phí xuất bản: Miễn phí
Thời gian phản biện: 50 ngày
Lập chỉ mục (Indexed): Google Scholar, Scilit

SCAN ME

Tạp chí Phát triển Khoa học và Công nghệ - Kinh tế-Luật và Quản lý
ISSN: 2588-1051
Hình thức xuất bản: In & trực tuyến
Hình thức truy cập: Truy cập mở
Ngôn ngữ bài báo: Tiếng Việt
Tỉ lệ chấp nhận đăng 2021: 65%
Phí xuất bản: Miễn phí
Thời gian phản biện: 45 ngày
Lập chỉ mục (Indexed): Google Scholar, Scilit

SCAN ME

Tạp chí Phát triển Khoa học và Công nghệ - Khoa học Xã hội và Nhân văn
ISSN: 2588-1043
Hình thức xuất bản: In & trực tuyến
Hình thức truy cập: Truy cập mở
Ngôn ngữ bài báo: Tiếng Việt
Tỉ lệ chấp nhận đăng 2021: 62%
Phí xuất bản: Miễn thu phí đối với tác giả là CBVC của ĐHKHXHNV, ĐHQG-HCM; Tác giả khác: 500.000 VNĐ/bài
Thời gian phản biện: 75 ngày
Lập chỉ mục (Indexed): Google Scholar, Scilit

SCAN ME

Tạp chí Phát triển Khoa học và Công nghệ - Khoa học Trái đất và Môi trường
ISSN: **2588-1078**
Hình thức xuất bản: In & trực tuyến
Hình thức truy cập: Truy cập mở
Ngôn ngữ bài báo: Tiếng Việt và tiếng Anh
Tỉ lệ chấp nhận đăng 2021: 87%
Phí xuất bản: liên hệ tòa soạn
Thời gian phản biện: 45 ngày
Lập chỉ mục (Indexed): Google Scholar, Scilit

SCAN ME

Tạp chí Phát triển Khoa học và Công nghệ - Khoa học Sức khỏe
ISSN: 2734-9446
Hình thức xuất bản: In & trực tuyến
Hình thức truy cập: Truy cập mở
Ngôn ngữ bài báo: Tiếng Việt
Tỉ lệ chấp nhận đăng 2021: 70%
Phí xuất bản: Miễn phí
Thời gian phản biện: 30 ngày
Lập chỉ mục (Indexed): Google Scholar, Scilit

SCAN ME

Tạp chí Phát triển Khoa học và Công nghệ, Đại học Quốc gia Tp.HCM
25 năm xuất bản học thuật (1997-2022)
Tòa soạn: Nhà điều hành Đại học Quốc gia Tp.HCM, P. Linh Trung, TP. Thủ Đức, TP. HCM
Email: stdj@vnuhcm.edu.vn; tcptkhcn@vnuhcm.edu.vn; Website: *http://www.scienceandtechnology.com.vn*